3764–3776 *Nucleic Acids Research, 2022, Vol. 50, No. 7* *Published online 22 March 2022*
https://doi.org/10.1093/nar/gkac179

Telomerase RNA TERC and the PI3K-AKT pathway form a positive feedback loop to regulate cell proliferation independent of telomerase activity

Shu Wu [1,†], Yuanlong Ge [1,2,*,†], Kaixuan Lin[3], Qianqian Liu[4], Haoxian Zhou[5], Qian Hu[1], Yong Zhao[5,‡], Weifeng He [6,*] and Zhenyu Ju[1,*]

[1]Key Laboratory of Regenerative Medicine of Ministry of Education, Institute of Aging and Regenerative Medicine, Jinan University, Guangzhou 510632, China, [2]GCH Regenerative Medicine Group-Jinan University Joint Research and Development Center, Jinan University, Guangzhou 510632, China, [3]Department of Genetics and Yale Stem Cell Center, Yale School of Medicine, New Haven, CT 06520, USA, [4]First Affiliated Hospital, School of Medicine, Jinan University, Guangzhou 510632, China, [5]MOE Key Laboratory of Gene Function and Regulation, State Key Laboratory of Biocontrol, School of Life Sciences, Sun Yat-sen University, Guangzhou 510006, China and [6]Institute of Burn Research, Southwest Hospital, State Key Laboratory of Trauma, Burn and Combined Injury, Chongqing Key Laboratory for Disease Proteomics, Army Military Medical University, Chongqing 400038, China

Received September 29, 2021; Revised February 11, 2022; Editorial Decision March 04, 2022; Accepted March 16, 2022

ABSTRACT

The core catalytic unit of telomerase comprises telomerase reverse transcriptase (TERT) and telomerase RNA (TERC). Unlike TERT, which is predominantly expressed in cancer and stem cells, TERC is ubiquitously expressed in normal somatic cells without telomerase activity. However, the functions of TERC in these telomerase-negative cells remain elusive. Here, we reported positive feedback regulation between TERC and the PI3K-AKT pathway that controlled cell proliferation independent of telomerase activity in human fibroblasts. Mechanistically, we revealed that TERC activated the transcription of target genes from the PI3K-AKT pathway, such as PDPK1, by targeting their promoters. Overexpression of PDPK1 partially rescued the deficiency of AKT activation caused by TERC depletion. Furthermore, we found that FOXO1, a transcription factor negatively regulated by the PI3K-AKT pathway, bound to TERC promoter and suppressed its expression. Intriguingly, TERC-induced activation of the PI3K-AKT pathway also played a critical role in the proliferation of activated CD4⁺ T cells. Collectively, our findings identify a novel function of TERC that regulates the PI3K-AKT pathway via positive feedback to elevate cell proliferation independent of telomerase activity and provide a potential strategy to promote CD4⁺ T cells expansion that is responsible for enhancing adaptive immune reactions to defend against pathogens and tumor cells.

INTRODUCTION

Normal somatic cells have a proliferative limit due to the end replication problem (1), which can be overcome in the majority of human tumor cells by activating telomerase, a ribonucleoprotein that maintains telomere length by the addition of telomeric TTAGGG repetitive sequences to the telomere ends (2). The telomerase complex consists of two main components: TERT, the telomerase reverse transcriptase subunit and TERC, the RNA template for reverse transcription (3,4). TERT transcription is epigenetically silenced in normal somatic cells; nevertheless, it is highly activated in tumor cells and stem cells. Conversely, TERC, the RNA template, is ubiquitously expressed in human tissue and cells, regardless of whether it harbors telomerase activity (5–7), implying that TERC has noncanonical functions beyond telomerase activity. Recent studies have revealed that TERC is involved in immune cells antiapoptotic effects, the DNA damage response and telomere length maintenance, in a manner that is independent of its telomere templating function (8–10). It was also reported that TERC stimulates the NF-κB (Nuclear factor-kappa B) pathway and increases the expression and secretion of inflammatory cytokines in telomerase-negative cells (11). In addition,

*To whom correspondence should be addressed. Tel: +86 2085224362; Email: zhenyuju@163.com
Correspondence may also be addressed to Yuanlong Ge. Tel: +86 2085224362; Email: geyuanlong@jnu.edu.cn.
Correspondence may also be addressed to Weifeng He. Tel: +86 2368765949; Email: whe761211@hotmail.com
†The authors wish it to be known that, in their opinion, the first two authors should be regarded as Joint First Authors.
‡Deceased on 8 April 2021.

Cheng *et al*. reported that TERC can be imported into mitochondria and processed to a shorter form TERC-53 that plays a regulatory role in cellular senescence, which is responsible for cognitive decline in 10-month-old mice, independent of its telomerase function (12,13). However, the functions of TERC in normal somatic cells remain elusive.

The PI3K-AKT pathway is an intracellular signaling pathway that is associated with multiple important cellular processes, including proliferation, metabolism, cell survival, protein synthesis and angiogenesis (14,15). The central mediator of the PI3K-AKT signaling pathway is a serine-threonine kinase, AKT, which serves as an indispensable conduit for the transmission of growth and survival signals from cell surface receptors (16). AKT has three conserved isoforms in mammalian cells, AKT1 (PKB α), AKT2 (PKB β) and AKT3 (PKB γ), which share homologous amino acid sequences, including the N-terminal regulatory region, kinase catalytic domain and C-terminal regulatory domain (17). Once PI3K is activated by extracellular signals, it catalyzes the phosphorylation of PI(4,5)P2 to form PI(3,4,5)P3, which then recruits AKT from the cytoplasm to the cell plasma membrane (18). Upon membrane recruitment, AKT is phosphorylated by PDPK1 at Thr308 located in the catalytic core domain, leading to AKT activation. Further phosphorylation at Ser473 located in the C-terminal regulatory domain by mTORC2 is responsible for full activation of AKT (19,20). Then, activated AKT moves to the cytoplasm and nucleus and phosphorylates numerous downstream effectors to modulate cell proliferation, metabolism, survival and motility (17). GSK3 and FOXOs, the two-best established downstream targets of AKT, act as the key signaling nodes to achieve diverse regulatory functions of the PI3K-AKT pathway (17).

In this study, we reported that depletion of TERC results in slowed or stopped proliferation independent of telomerase activity in normal somatic cells. Mechanistic study showed that PI3K-AKT signaling was down-regulated by TERC depletion through transcriptional regulation of target genes from the PI3K-AKT signaling pathway. Furthermore, we found that a key transcription factor FOXO1, which was negatively regulated by the PI3K-AKT pathway, bound to the TERC promoter and suppressed its transcription. Thus, it suggested a positive feedback loop between TERC and the PI3K-AKT pathway. In addition, we found that TERC-mediated PI3K-AKT signaling activation plays a critical role in the proliferation of activated $CD4^+$ T cells. Both AKT and/or PDPK1 inhibitors blocked the elevated proliferation of activated $CD4^+$ T cells induced by TERC. Together, our findings identify a novel function of TERC to elevate cell proliferation through a positive feedback loop with the PI3K-AKT pathway independent of telomerase activity, which may act as a potential mechanism for $CD4^+$ T cells expansion during adaptive immune reactions to defend against infectious pathogens and tumor cells.

MATERIALS AND METHODS

Cell culture and compounds

MRC5 fibroblast cells, BJ fibroblast cells were obtained from American Type Culture Collection (ATCC). 293T were purchased from Chinese Academy of Sciences of Type Culture Collection (CTCC). Cells were cultured in DMEM medium (Gibco) with 10% fetal bovine serum (Gibco) and 100 U/ml penicillin/ streptomycin (Gibco). Negatively selected-$CD4^+$ T cells were directly purchased from Leidebio, Guang Zhou, China. For $CD4^+$ T activation, $CD4^+$ T cells were seeded at a density of 1×10^6 per well in 1 ml ImmunoCult™-XF T Cell Expansion Medium (Stemcell) and activated with 25 μl ImmunoCult Human CD3/CD28 T Cell Activator (Stemcell) and 10 ng/ml IL-2 (Stemcell) for 72 h followed by siRNA transfection, virus infection or drug treatment. These cell lines were maintained in a humidified chamber containing 5% CO_2 at 37 °C.

DMEM without glucose was purchased in Gibco. 2-Deoxy-D-glucose (2-DG), MK-2206, PHT-427, AS1842856 and BIBR1532 were purchased in Selleck.

Gene silence and overexpression

SiRNA was transfected into target cells using Lipofectamine RNAiMAX Transfection Reagent (Invitrogen), according to the manufacturer's instructions. siRNA against TERC (si-1: 5′-GUCUAACCCUAACUGAGAAGGdTdT-3′; si-2: 5′-CCGUUCAUUCUAGAGCAAACdTdT-3′), FOXO1 (si-1: 5′-GAGCGUGCCCUACUUCAAGdTdT-3′; si-2: 5′-UCUCCUAGGAGAAGAGCUGdTdT-3′), were provided by Suzhou GenePharma Co., Ltd. The scrambled sequence was used as a control.

FG12-puro lentiviral vector (abbreviated as FG12-EV) was reconstructed from FG12 (21) through replacing EGFP sequence by puromycin resistance gene (PuroR) sequence. U3-TERC cassette was amplified from pBABEpuro U3-TERC-500 (22) and cloned into FG12-puro vector to yield FG12-puro-TERC (abbreviated as FG12-TERC). PDPK1 gene was cloned into pLenti-Dest-EF1a-IRES-puro (abbreviated as pLenti-EV) to yield pLenti-Dest-EF1a-IRES-puro-PDPK1 (abbreviated as pLenti-PDPK1). Lentivirus was packaged in 293T cells using calcium phosphate transfection. The virus supernatants were harvested at 48 and 72 h after transfection, filtered with 0.45 μm filter unit (millipore) and stored at −80°C in aliquots. Cells were infected with lentivirus for 24 h and selected with puromycin (Sangon) before collection for further analysis at indicated times. Plasmids were transfected into MRC5 cells by 4D-Nucleofector system (Lonza).

EdU staining assay

MRC5 and BJ cells on the coverslip were cultured with medium supplemented with 10 μM EdU for indicated times (MRC5 cells for 2 h and BJ cells for 4 h, respectively). Then, cells were washed with PBS and fixed with 4% paraformaldehyde for 15 min at room temperature. Following incubation, the fixed cells were permeabilized with 0.3% Triton X-100 (in 1× PBS) for 15 min at room temperature. Cells were stained at room temperature for 30 min with staining buffer (10 μM FAM-azide, 1 mM $CuSO_4$ and 10 mM sodium ascorbate in PBS), then washed and mounted with DAPI. Fluorescence was detected and imaged using Zeiss Axion Imager Z1 microscope.

TERC ChIRP assay

ChIRP assay were performed as previously described using odd probes of TERC and LacZ (23,24). Briefly, 40 million MRC5 cells were collected and fixed with 1% glutaraldehyde in PBS for 10 min at room temperature, reflection terminated by 1.25 mM glycine for 5 min. Cells were washed twice with chilled PBS, and re-suspended in lysis buffer (50 mM Tris 7.0, 10 mM EDTA, 1% SDS, add DTT, PMSF, P.I., and Superase-in before use), and sonicated in a 4°C water bath to bulk of the DNA smear is 100–500 bp in size. The supernatant was collected, and diluted with 2 times volume of hybridization buffer (500 mM NaCl, 1%SDS, 100 mM Tris 7.0, 10 mM EDTA, 15% formamide, add DTT, PMSF, P.I, and Superase-in fresh) and appropriate volume of probes (TERC odd probes or Laz-probe), incubated at 37°C for 4 h with shaking. Streptavidin-magnetic C1 beads were blocked with 500 ng/μl yeast total RNA and 1 mg/ml BSA for 1 h at room temperature, and resuspended with original volume of lysis buffer and added to the hybridization system, 37°C for 30 min with shaking. Then, Streptavidin-magnetic C1 beads were washed five times with wash buffer (2 × SSC, 0.5% SDS, add DTT and PMSF fresh). For DNA elution, beads were resuspended in 3 × original volume DNA elution buffer (50 mM $NaHCO_3$, 1% SDS, 200 mM NaCl) with RNase A and RNase H, followed by reverse cross-linking, proteinase K digestion and phenol-chloroform extraction. DNA fragments were precipitated by ethanol in the presence of NaAc and glycogen. Eluted DNA was subject to PCR and high-throughput sequencing.

TERC ChIRP-seq Analysis

High-throughput sequencing was carried out in Sangon Biotech using Illumina Hiseq. High-quality raw reads were aligned to the human genome (UCSC, hg38) with Bowtie2 (v2.3.1, default settings) (25). Bigwig signal tracks were generated using DeepTools (v3.1.3) (26) and normalized to reads per genomic content (RPGC). Aggregation profiles and heatmaps were generated from bigwig files of TERC-ChIRP and Input over hg38 refGenes using DeepTools. Peaks were called using MACS14, and categorical annotation of peaks on genomic elements was performed using CEAS (27). Significant peaks were identified with the setting of Enrichment Fold > 3 and *P*-value < 0.0001. KEGG pathway enrichment analysis was performed using DAVID (28,29).

Quantitative real-time PCR

Total RNA was extracted from cells using RNAiso Plus Reagent (Takara) according to manufacturer's instructions. About 1.0 μg of total RNA was reverse-transcribed to cDNA using PrimeScript RT reagent Kit (Takara). cDNA was used for real-time PCR using 2 × RealStar Green Fast Mixture (GenStar). β-Actin was used as internal control. All PCR primers sequences were from Genecards (30).

Western blot

Cells were directly lysed in 2 × SDS loading buffer and boiled for 10 min. Proteins were separated by SDS–PAGE, transferred to PVDF membrane and probed with antibodies specific for, p-S473 AKT (4060, Cell Signaling Technology), p-T308 AKT (13038, Cell Signaling Technology), AKT (ab32505, Abcam), p-S9 GSK3β (9322, Cell Signaling Technology), GSK3β (9315, Cell Signaling Technology), PDPK1 (ab52893, abcam), Flag (F1804, Sigma). β-Actin (66009–1-Ig, Proteintech) antibody was used as a loading control. Samples derived from the same experiment and gels/blots were processed in parallel.

Chromatin immunoprecipitation

Cells were cross-linked with 1% formaldehyde, and terminated by 1.25 mM Glycine, after washed twice with cold PBS, cells were resuspended in SDS lysis buffer (50 mM Tris–HCl, pH 8.1, 10 mM ethylenediaminetetraacetic acid, 1% SDS) and sonicated. The supernatant was precleared with Protein-A/G agarose beads precoated with *Escherichia coli* genomic DNA. Chromatin immunoprecipitation (ChIP) was carried out overnight at 4 °C with primary antibodies against FOXO1 (1:100 dilution, 2880, Cell Signaling Technology), or IgG (Sangon). Beads were washed three times, and eluted with 0.1 M $NaHCO_3$ and 1% SDS, followed by reverse cross-linking and phenol-chloroform extraction. DNA fragments were precipitated by ethanol in the presence of NaAc and glycogen. PCR was carried out to identify DNA fragment enriched in complexes. The following primers were used to detect the fragments of TERC promoters: pTERC-TS-forward: 5′-GAGAGAGTGACTCTCACGAGAGC-3′; pTERC-TS-reverse: 5′-CGAGTCGGCTTATAAAGGGAGCG-3′; pTERC-1K-forward: 5′-CCACGGAGTTTATCTAACTGAATACGAG-3′; pTERC-1K-reverse: 5′-AAAGTGCTGGGATTACAGGTATGAGC-3′; pTERC-2K-forward: 5′-GTCCCAGGCTGGAGTGCAGT-3′; pTERC-2K-reverse: 5′-GCATACCTGTGGATTCAGTTACTTGGG-3′.

TRAP assay

TRAP assay was performed as described previously (31,32). Samples were resolved by PAGE gel and scanned using Tannon Gel Image System.

Statistical analysis

All statistical analyses were performed using GraphPad Prism software (Version 8). Data are presented as the mean and standard deviation of at least three independent experiments. *P*-Value were calculated by Student's two-tailed *t*-test, one- or two-way ANOVA as indicated in the figure legends. For ANOVA, adjustments were made for multiple comparisons by Dunnett or Tukey corrections as appropriate. Exact P-values can be found in the figure legends.

RESULTS

TERC deficiency induces decelerated proliferation in normal somatic cells independent of telomerase activity

To explore the function of TERC in normal somatic cells without telomerase activity, we depleted TERC in MRC5

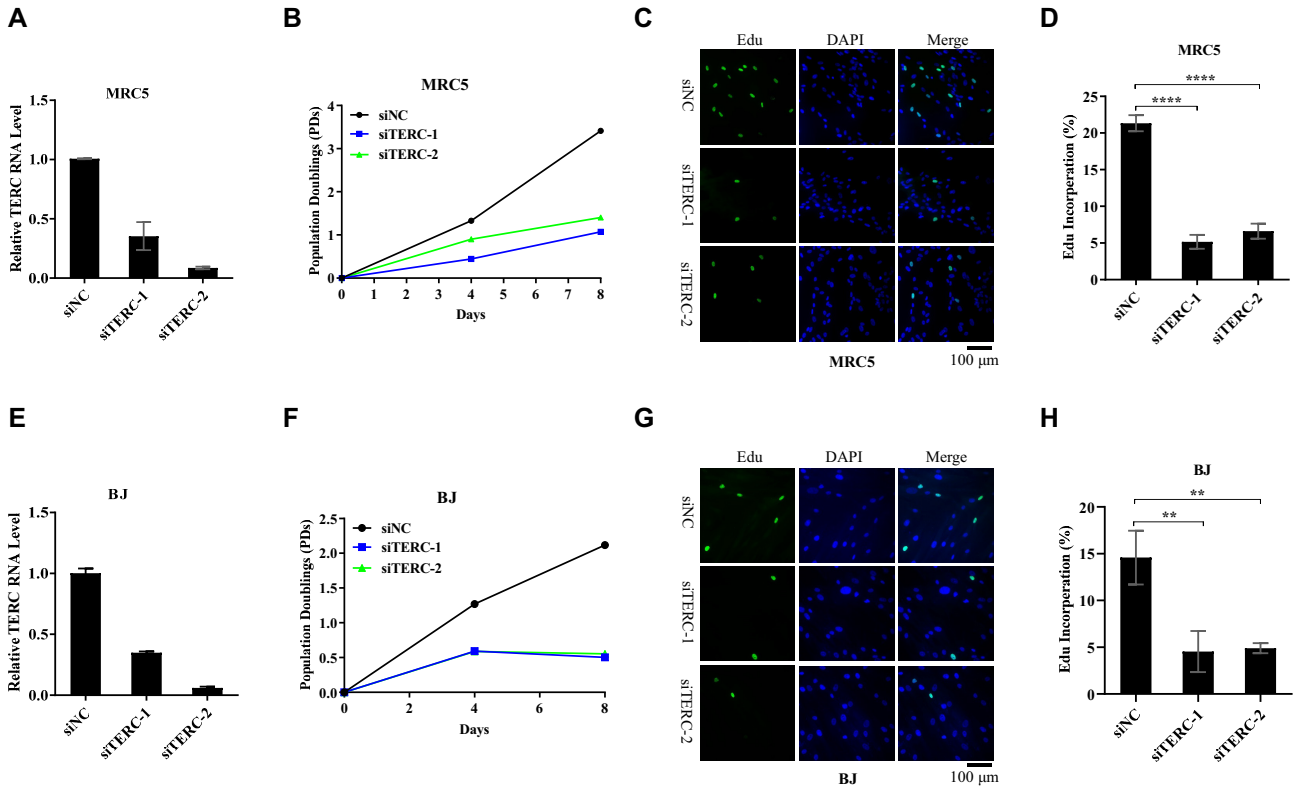

Figure 1. TERC depletion decelerates cell proliferation in MRC5 and BJ fibroblast cells. (**A**) The RNA level of TERC in the control and the TERC-depleted MRC5 cells. MRC5 cells were transfected with two distinct siRNAs target to TERC for 72 h, qPCR analysis of TERC knockdown efficiency. (**B**) Proliferation of the control and the TERC-depleted MRC5 cells. MRC5 cells were transfected with siRNAs for 8 days, cell PDs (Population Doublings) were used to estimate cell growth. (**C**) Edu assay of the control and the TERC-depleted MRC5 cells. MRC5 cells transfected with siRNAs for 72 h and then labeled with 10 μM EdU for 2 h. The incorporation of EdU was determined by fluorescence microscope. (**D**) Quantification of the data in (C), data represent the mean ± SD of three independent experiments, significance was determined using one-way ANOVA with Dunnett's test, $^{****}P < 0.0001$. (**E**) The RNA level of TERC in the control and the TERC-depleted BJ cells. BJ cells were transfected with two distinct siRNAs target to TERC for 72 h, qPCR analysis of TERC knockdown efficiency. (**F**) Proliferation of the control and the TERC-depleted BJ cells. BJ cells were transfected with siRNAs for 8 days, and cell PDs (population doublings) were used to estimate cell growth. (**G**) Edu assay of the control and the TERC-depleted BJ cells. BJ cells transfected with siRNAs for 72 h and then labeled with 10 μM EdU for 4 h. The incorporation of EdU was determined by fluorescence microscope. (**H**) Quantification of the data in (G), data represent the mean ± SD of three independent experiments, significance was determined using one-way ANOVA with Dunnett's test, $^{**}P = 0.002$ (siTERC-1) and 0.0024 (siTERC-2) compared with siNC.

fibroblast cells with two distinct siRNAs (Figure 1A), and the rates of cell proliferation were evaluated by population doublings (PDs). Our results showed that knockdown of TERC led to a significant deceleration of proliferation in the TERC-depleted cells (Figure 1B). Moreover, the EdU staining assay showed that the TERC-depleted cells displayed a lower EdU incorporation rate than the control cells (Figure 1C,D). These results were also confirmed in BJ fibroblast cells (Figure 1E–H). All these results indicated that TERC depletion decelerates cell proliferation in normal somatic cells independent of telomerase activity.

TERC occupies genomic sites enriched in the PI3K-AKT signaling pathway

TERC is a typical lncRNA that was reported to occupy telomeres and Wnt pathway genes in HeLa S3 cells transduced with TERC and TERT (23). Recently, García-Castillo *et al.* have shown that TERC binds to specific DNA sequences of master myeloid genes and controls their expression through recruiting RNA polymerase II in Zebrafish (33). To explore how TERC regulates cell proliferation in normal somatic cells, we performed ChIRP-seq (Chromatin Isolation by RNA Purification Followed by Sequencing) to identify the genomic binding sites of TERC in MRC5 fibroblast cells (Figure 2A and Supplementary Table S1). Strikingly, we did not find a strong enrichment of TERC on telomeric sequences over 'Input' in MRC5 cells (Figure 2B), which is inconsistent with the observation in HeLa cells, thus further supporting that TERT is essential for the localization of TERC to telomeres (34). In addition, we observed that most of the peak sizes of TERC were <600 bp, which is a pattern reminiscent of sharp peaks from transcription factors (Figure 2C). Then, we analyzed the genomic targets of TERC in MRC5 cells and observed a strong enrichment near the gene promoter, mostly adjacent to the transcription start site (TSS) (Figure 2D,E). Further analysis of the significant TERC-bound peaks revealed that one of the top three enriched KEGG pathways

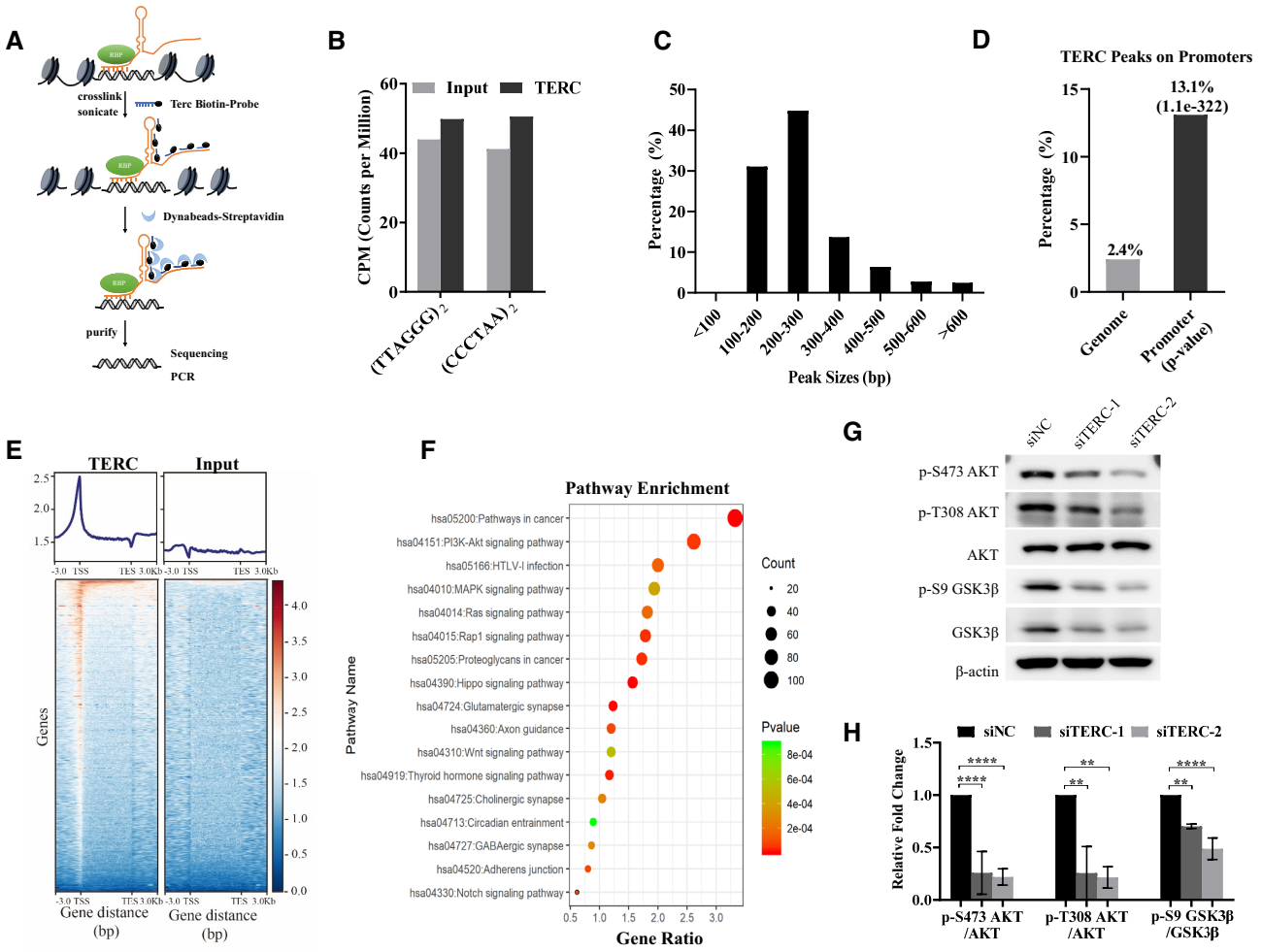

Figure 2. TERC occupies genomic sites enrich in the PI3K-AKT signaling pathway. (**A**) A schematic diagram of ChIRP protocol. Chromatin is cross-linked, fragmented, and hybridized to TERC-biotinylated probes. TERC-bound DNA were purified for DNA sequencing or PCR detection. (**B**) Counts per million of reads from TERC-ChIRP and Input samples that map to telomere sequences. Reads from 'TERC ChIRP' sample and 'Input' sample were compared against telomere sequence $(TTAGGG)_2$ and $(CCCTAA)_2$. (**C**) Histogram distribution of peak sizes from TERC ChIRP-seq. (**D**) Bar chart showing the percentage of TERC ChIRP-seq peaks on promoters. *P*-value computed versus genome random. (**E**) Average signal and heatmaps of TERC ChIRP-seq and Input over hg38 reference genes. (**F**) KEGG pathway analysis of genes with significant TERC ChIRP-seq peaks. (**G**) TERC depletion decreased AKT activation in MRC5 cells. The control and the TERC-depleted MRC5 cells were collected for western blotting of indicated proteins. (**H**) Quantification of the data in (G), data represent the mean ± SD of three independent experiments, significance was determined using one-way ANOVA with Dunnett's test, for p-S473 AKT/AKT: $^{****}P < 0.0001$; for p-S308 AKT/AKT: $^{**}P = 0.0023$ (siTERC-1) and 0.0017 (siTERC-2) compared with siNC; for p-S9 GSK3β/GSK3β: $^{**}P = 0.0018$, $^{****}P < 0.0001$.

was the PI3K-AKT signaling pathway ($P = 3.9 \times 10^{-5}$) (Figure 2F).

To determine the effect of TERC on the PI3K-AKT signaling pathway, we focused on AKT, the central mediator of the PI3K-AKT signaling pathway. It is known that AKT is fully activated through phosphorylation at Thr308 and Ser473 sites (19,20). Then, we knocked down TERC in MRC5 and BJ cells, and observed a significantly decreased level of AKT phosphorylation at Thr308 and Ser473 sites. This result was consistent with the decreased phosphorylation of the AKT downstream effector GSK3β, which can act as a surrogate measure of AKT catalytic activity (Figure 2G,H and Supplementary Figure S1). These data confirmed that TERC is involved in the regulation of the PI3K-AKT signaling pathway.

TERC functions in the PI3K-AKT signaling pathway through modulating gene transcription

To determine how TERC impacts the PI3K-AKT pathway, we analyzed TERC-occupied genes from ChIRP-Seq that are associated with the PI3K-AKT pathway. Based on the results in Figure 2D,E, we identified 38 genes with TERC binding peaks at the promoters/TSS regions. Then, we knocked down TERC in MRC5 cells, and used qPCR to detect the mRNA levels of these genes. The results in Figure 3A showed that the mRNA levels of seven genes (COL24A1, COL5A1, EGFR, IL4R, PDPK1, PRKCA, TNXB) were suppressed or induced by TERC depletion. Then, we detected the mRNA levels of these seven genes in the TERC-depleted BJ cells and found that the mRNA levels of four genes (EGFR, IL4R, PDPK1, PRKCA) were

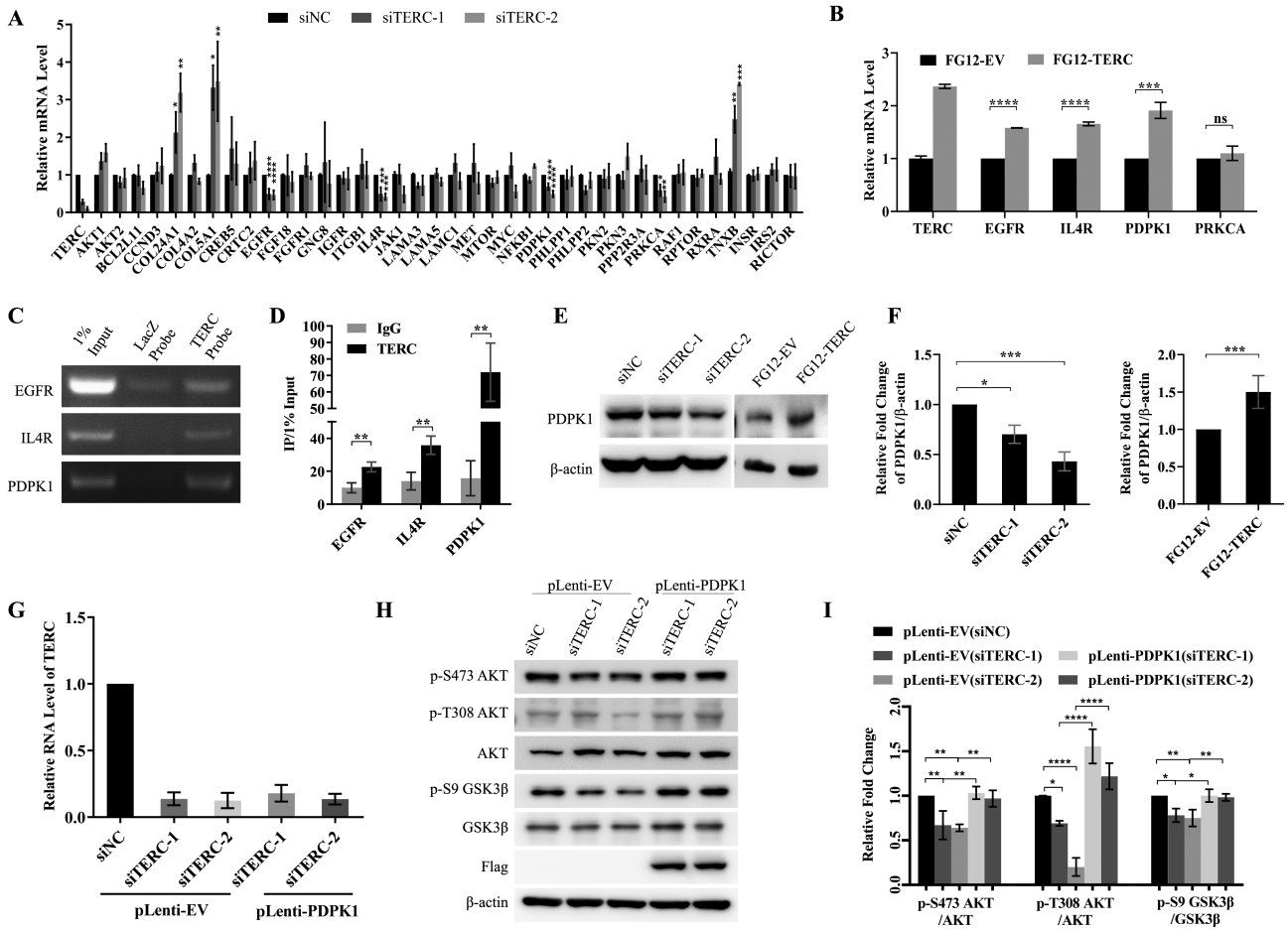

Figure 3. TERC is involved in the PI3K-AKT pathway through gene transcriptional regulation. (**A**) The mRNA levels of 38 genes from PI3K-AKT pathway with TERC-ChIRP peaks in the promoters/TSS regions in the control and the TERC-depleted MRC5 cells. MRC5 cells were transfected with two distinct siRNAs target to TERC for 48 h, qPCR analysis of TERC knockdown efficiency and the mRNA levels of 38 genes. Data represent the mean ± SD of three independent experiments, significance was determined using one-way ANOVA with Dunnett's test, for COL24A1: $*P = 0.0330$, $**P = 0.0015$; for COL5A1: $*P = 0.0122$, $**P = 0.0088$; for EGFR: $****P < 0.0001$; for IL4R: $***P = 0.0003$ (siTERC-1) and 0.0001 (siTERC-2) compared with siNC; for PDPK1: $****P < 0.0001$; for PRKCA: $*P = 0.0111$, $**P = 0.0022$; for TNXB: $**P = 0.0014$, $***P = 0.0002$. (**B**) The mRNA levels of four screened genes in the control and the TERC-overexpressed MRC5 cells. qPCR analysis of TERC overexpression efficiency and the mRNA levels of four screened genes in MRC5 cells with the expression of FG12-EV or FG12-TERC. Data represent the mean ± SD of three independent experiments, significance was determined using two-tailed Student's *t*-test, $****P < 0.0001$, $***P = 0.0005$, ns = 0.2754. (**C**) PCR of TERC-immunoprecipitated chromatin for screened genes' promoter in MRC5 cells. (**D**) Quantification of the data in (C), data represent the mean ± SD of three independent experiments, significance was determined using two-tailed Student's *t*-test, for EGFR: $**P = 0.0065$; for IL4R: $**P = 0.0081$; for PDPK1: $**P = 0.0016$. (**E**)TERC depletion decreased PDPK1 expression and TERC overexpression induced PDPK1 expression in MRC5 cells. The control and the TERC-depleted or -overexpressed MRC5 cells were collected for western blotting of indicated proteins. (**F**) Quantification of the data in (E), data represent the mean ± SD of three independent experiments, significance was determined using one-way ANOVA with Dunnett's test or two-tailed Student's *t*-test, TERC knockdown: $*P = 0.0297$, $***P = 0.0004$; TERC overexpression: $***P = 0.0009$. (**G**) Expression of TERC in the TERC-depletion MRC5 cells with exogenous PDPK1. TERC was knocked down in the control and the PDPK1-overexpressed MRC5 for 72 h, qPCR analysis of TERC knockdown efficiency. (**H**) PDPK1 reversed TERC depletion-induced decrease of AKT phosphorylation level. Cells were treated as shown in (G), and collected for western blotting of indicated proteins. (**I**) Quantification of the data in (H), data represent the mean ± SD of three independent experiments, significance was determined using one-way ANOVA with Tukey's test, for p-S473 AKT/AKT: $**P = 0.0078$ (pLenti-EV(siNC) versus pLenti-EV(siTERC-1)), 0.0044 (pLenti-EV(siNC) versus pLenti-EV(siTERC-2)), 0.0041 (pLenti-EV(siTERC-1) versus pLenti-PDPK1(siTERC-1)) and 0.0082 (pLenti-EV(siTERC-2) versus pLenti-PDPK1(siTERC-2)); for p-S308 AKT/AKT: $*P = 0.0376$, $****P < 0.0001$; for p-S9 GSK3β/GSK3β: $*P = 0.0135$ (pLenti-EV(siNC) versus pLenti-EV(siTERC-1)) and 0.0057 (pLenti-EV(siTERC-1) versus pLenti-PDPK1(siTERC-1)), $**P = 0.0057$ (pLenti-EV(siNC) versus pLenti-EV(siTERC-2)) and 0.0094 (pLenti-EV(siTERC-2) versus pLenti-PDPK1(siTERC-2)).

consistently downregulated by TERC depletion (Supplementary Figure S2A). Conversely, the TERC-overexpressed MRC5 and BJ cells showed increased mRNA levels of three out of four genes (EGFR, IL4R, PDPK1) (Figure 3B and Supplementary Figure S2B). Moreover, we observed enrichment of TERC at the promoter region of these three genes by ChIRP-PCR (Figure 3C,D), raising the intriguing possibility that TERC regulates the transcription of these genes by targeting their promoters.

Among them, PDPK1 is the key regulator for AKT activation (19). It was speculated that TERC modulates AKT activation through regulation of PDPK1 expression. To fur-

ther test this hypothesis, we measured the protein level of PDPK1 with TERC depletion or overexpression. The results showed that depletion of TERC resulted in a significant decrease of cellular PDPK1 protein level while overexpression of TERC resulted in significant increase of cellular PDPK1 protein level in both MRC5 and BJ cells (Figure 3E,F; Supplementary Figure S2C and D). To verify the critical role of PDPK1 in the modulation of AKT activation by TERC, we exogenously expressed PDPK1 in the TERC-depleted cells and found that compensatory expression of PDPK1 significantly reversed the decreased phosphorylation of AKT and GSK3β (Figure 3G–I). These results indicate that TERC regulates AKT activation mainly through PDPK1.

Activated AKT modulates TERC transcriptional expression through FOXO1

AKT was reported to be the major signal regulator for maintaining cell proliferation and survival in response to various growth factors and diverse stresses, such as metabolic stress and oxidative stress (35). However, whether activated AKT can induce TERC expression is still unclear. Then we used EGF, glucose deprivation stress (glucose starvation, 2-DG) and oxidative stress (H_2O_2) to treat MRC5 at the indicated times, which induced AKT activation (Figure 4A,B). Intriguingly, we observed that all these treatments significantly induced TERC expression (Figure 4C–F). Activated AKT elevates TERC expression, while TERC depletion decelerates AKT activation, which indicates that there is positive feedback between activated AKT and TERC expression.

To define how activated AKT regulates TERC expression, we used the Eukaryotic Promoter Database (EPD) (36) to predict the potential transcription factor motifs in the promoter region of TERC. We observed that FOXO1, an important transcription factor downstream of the PI3K-AKT pathway, may bind to the promoter region of TERC (-1211 bp relative to the transcription start site) with a cut-off *P*-value of 0.0001 (Figure 4G). As a transcription factor, FOXO1 has been reported to play critical roles in cellular homeostasis, including energy metabolism, oxidative stress resistance and cell viability and proliferation, and activated PI3K-AKT signaling leads to its translocation out of the nucleus and attenuation of its transcriptional program (37–39). We wondered whether activated AKT regulates TERC expression through FOXO1. Thus, we knocked down FOXO1 with two different siRNAs in both MRC5 and BJ cells, and found that TERC RNA level was specifically increased (Figure 4H,I; Supplementary Figure S3A and B). Meanwhile, TERC RNA level was also obviously increased in MRC5 and BJ cells following FOXO1 inhibitor (AS1842856) treatment (Figure 4J and Supplementary Figure S3C). Then, we performed ChIP assay followed by PCR to demonstrate the interaction between FOXO1 and the TERC promoter, and found that FOXO1 was enriched on the TERC promoter located 1–2 kb upstream of its TSS (Figure 4K and L). These results strongly suggested that AKT regulates TERC RNA levels through the transcription factor FOXO1.

TERC regulates the proliferation of activated CD4$^+$ T cells by targeting to AKT independent of telomerase activity

Cell proliferation is a key feature of adaptive immune responses. To act as an antipathogenic response, CD4$^+$ T cells must undergo rapid cell proliferation, and monitoring CD4$^+$ T cell proliferation is essential for the evaluation of adaptive immune reactions (40). It has been reported that TERC expression is up-regulated significantly in peripheral blood CD4$^+$ T cells after *in vitro* activation (41). We found that CD4$^+$ T cells proliferated rapidly, TERC expression was up-regulated significantly after activation, and the proliferation rate of activated CD4$^+$ T cells slowed down accompanied by a decline in the expression of TERC (Figure 5A,B).

During the process of T cell activation, CD28-dependent recruitment and activation of PI3K can result in the intracellular accumulation of 3-phosphorylated lipids that can bind and induce the phosphorylation of pleckstrin homology domain-containing proteins for activation (42,43), such as AKT. Upon activation, T cells undergo multiple rounds of proliferation, which is an energy-consuming process that entails dramatic changes in cellular metabolism to produce high level of adenosine 5′-triphosphate (ATP) accompanied by the by-products reactive oxygen species (ROS) (44,45). As shown in Figure 4A and F, H_2O_2-induced oxidative stress activated AKT and elevated the expression of TERC. Then, we detected AKT phosphorylation level during the proliferation of activated CD4$^+$ T cells and found that the phosphorylation of AKT was also up-regulated significantly after activation, and a decreased phosphorylation level of AKT accompanied by a decline in the TERC expression was observed (Figure 5C,D).

It is speculated that TERC and activated AKT may also play important roles in CD4$^+$ T cell proliferation. To determine our hypothesis, we knocked down TERC in activated CD4$^+$ T cells (Figure 5E), and found that the TERC-depleted cells displayed a slower proliferation rate than the control cells (Figure 5F), while the TERC-overexpressed activated CD4$^+$ T cells showed a faster proliferation rate than EV-expressed cells (Figure 5G,H). These results are consistent with the results in MRC5 and BJ cells. Furthermore, we detected the phosphorylation of AKT in the TERC-depleted or TERC-overexpressed activated CD4$^+$ T cells (Figure 5I,J); the results further supported the conclusion that TERC induces the activated level of AKT in cells. Then, we used AKT and/or PDPK1 inhibitors to treat the TERC-overexpressed activated CD4$^+$ T cells and observed that AKT and/or PDPK1 inhibition reversed the elevated proliferation and AKT activation induced by TERC overexpression (Figure 5K, Supplementary Figure S4A and B). Moreover, exogenous expression of PDPK1 completely counteracted the effects of decreased phosphorylation level of AKT and proliferation defects caused by TERC depletion (Supplementary Figure S4C–F). These results suggested that TERC-induced activation of AKT is critical for the proliferation of activated CD4$^+$ T cells.

It has been reported that telomerase inhibition with BIBR 1532 (an inhibitor of telomerase activity) has a direct cytotoxic effect in leukemia cells but not in normal hematopoietic stem cells and T cells (46,47). To exclude the

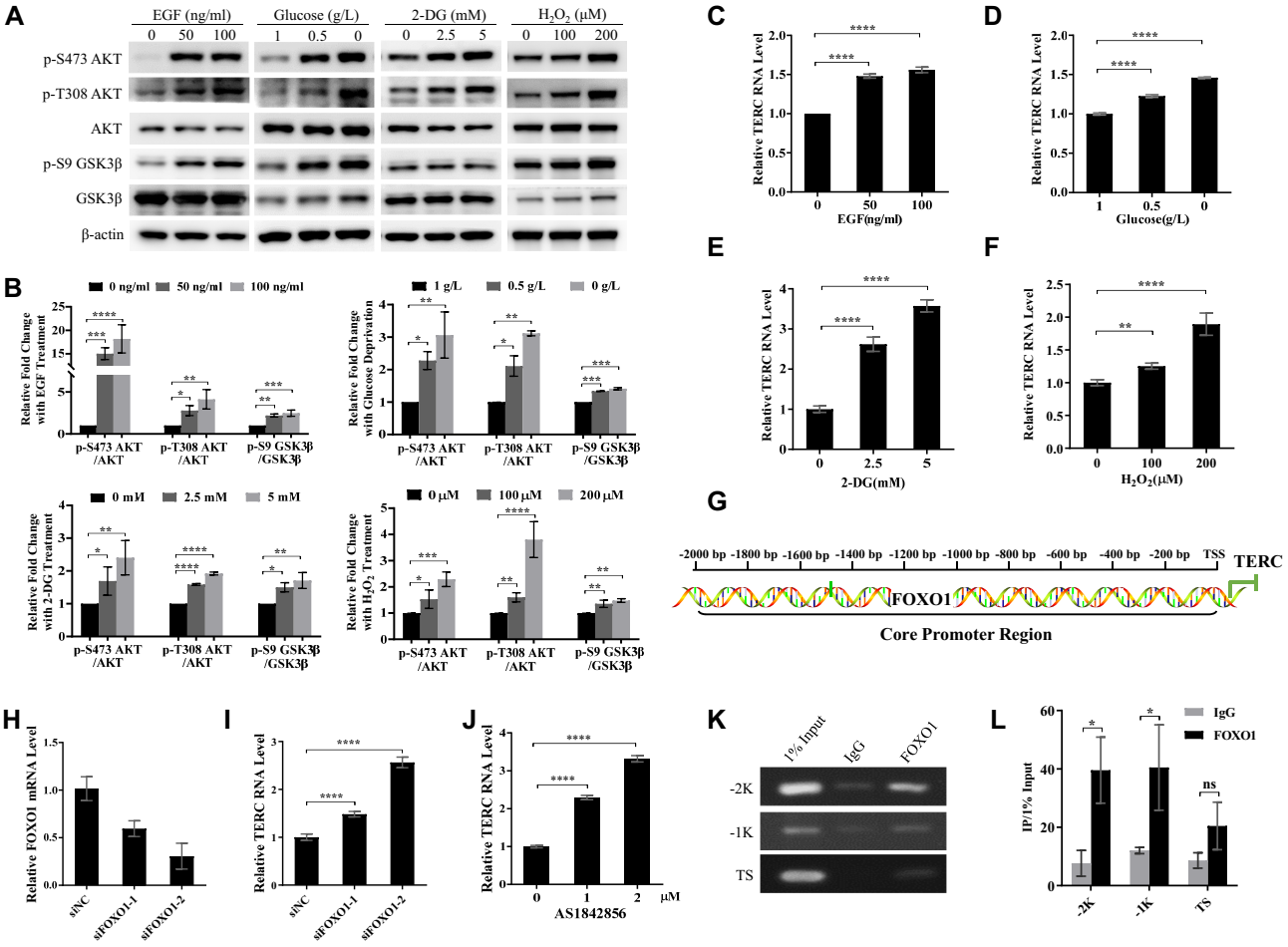

Figure 4. Activated AKT induces TERC expression through FOXO1. (**A**) EGF, glucose starvation, 2-DG and H_2O_2 induced AKT activation in MRC5 cells. MRC5 cells were treated with EGF (0, 50 and 100 ng/ml with serum starvation) for 15 min, different gradient glucose-containing medium (1, 0.5 and 0 g/L), 2-DG (0, 2.5 and 5 mM) or H_2O_2 (0, 100 and 200 μM) for 4 h, and collected for western blotting of indicated proteins. (**B**) Quantification of the data in (A), data represent the mean ± SD of three independent experiments, significance was determined using one-way ANOVA with Dunnett's test. EGF treatment: for p-S473 AKT/AKT: $***P = 0.0002$, $****P < 0.0001$; for p-S308 AKT/AKT: $*P = 0.0481$, $**P = 0.0041$; for p-S9 GSK3β/GSK3β: $**P = 0.0015$, $***P = 0.0005$. Glucose deprivation: for p-S473 AKT/AKT: $*P = 0.0212$, $**P = 0.0022$; for p-S308 AKT/AKT: $*P = 0.0157$, $**P = 0.0024$; for p-S9 GSK3β/GSK3β: $***P = 0.0007$ (0.5 g/L) and 0.0004 (0 g/L) compared with 1 g/L. 2-DG treatment: for p-S473 AKT/AKT: $*P = 0.0366$, $**P = 0.0026$; for p-S308 AKT/AKT: $****P < 0.0001$; for p-S9 GSK3β/GSK3β: $*P = 0.0127$, $**P = 0.0048$. H_2O_2 treatment: for p-S473 AKT/AKT: $*P = 0.0355$, $***P = 0.0004$; for p-S308 AKT/AKT: $**P = 0.0091$, $****P < 0.0001$; for p-S9 GSK3β/GSK3β: $**P = 0.0051$ (100 μM) and 0.0011 (200 μM) compared with 0 μM. (**C**) EGF induced TERC expression in MRC5 cells. MRC5 cells were serum starved and treated with EGF (0, 50 and 100 ng/ml) for 24 h, and collected for qPCR of TERC expression. Data represent the mean ± SD of three independent experiments, significance was determined using one-way ANOVA with Dunnett's test, $****P < 0.0001$. (**D**) Glucose deprivation induced TERC expression in MRC5 cells. MRC5 cells were cultured in 1, 0.5 and 0 g/L glucose-containing medium for 24 h, and collected for qPCR of TERC expression. Data represent the mean ± SD of three independent experiments, significance was determined using one-way ANOVA with Dunnett's test, $****P < 0.0001$. (**E**) 2-DG induced TERC expression in MRC5 cells. MRC5 cells were treated with 2-DG (0, 2.5 and 5 mM) for 24 h, and collected for qPCR of TERC expression. Data represent the mean ± SD of three independent experiments, significance was determined using one-way ANOVA with Dunnett's test, $****P < 0.0001$. (**F**) H_2O_2 induced TERC expression in MRC5 cells. MRC5 cells were treated with H_2O_2 (0, 100 and 200 μM) for 24 h, and collected for qPCR of TERC expression. Data represent the mean ± SD of three independent experiments, significance was determined using one-way ANOVA with Dunnett's test, $**P = 0.0025$, $****P < 0.0001$. (**G**) Schematic diagram of predicted FOXO1 binding site in TERC promoter. (**H**) The mRNA level of FOXO1 in the control and the FOXO1-depleted MRC5 cells. MRC5 cells were transfected with two distinct siRNAs target to FOXO1 for 72 h, qPCR analysis of FOXO1 knockdown efficiency. (**I**) The RNA level of TERC in the control and the FOXO1-depleted MRC5 cells. MRC5 cells were treated as shown in (H), qPCR analysis of TERC expression. Data represent the mean ± SD of three independent experiments, significance was determined using one-way ANOVA with Dunnett's test, $****P < 0.0001$. (**J**) The RNA level of TERC in the DMSO-treated and the AS1842856-treated MRC5 cells. MRC5 cells were treated with AS1842856 (0, 1 and 2 μM) for 24 h, and collected for qPCR analysis of TERC expression. Data represent the mean ± SD of three independent experiments, significance was determined using one-way ANOVA with Dunnett's test, $****P < 0.0001$. (**K**) PCR of FOXO1-immunoprecipitated chromatin for TERC promoter in MRC5 cells. (**L**) Quantification of the data in (K), data represent the mean ± SD of three independent experiments, significance was determined using two-tailed Student's *t*-test, for -2K: $*P = 0.0104$; for -1K: $*P = 0.0285$; for TS: ns = 0.0747.

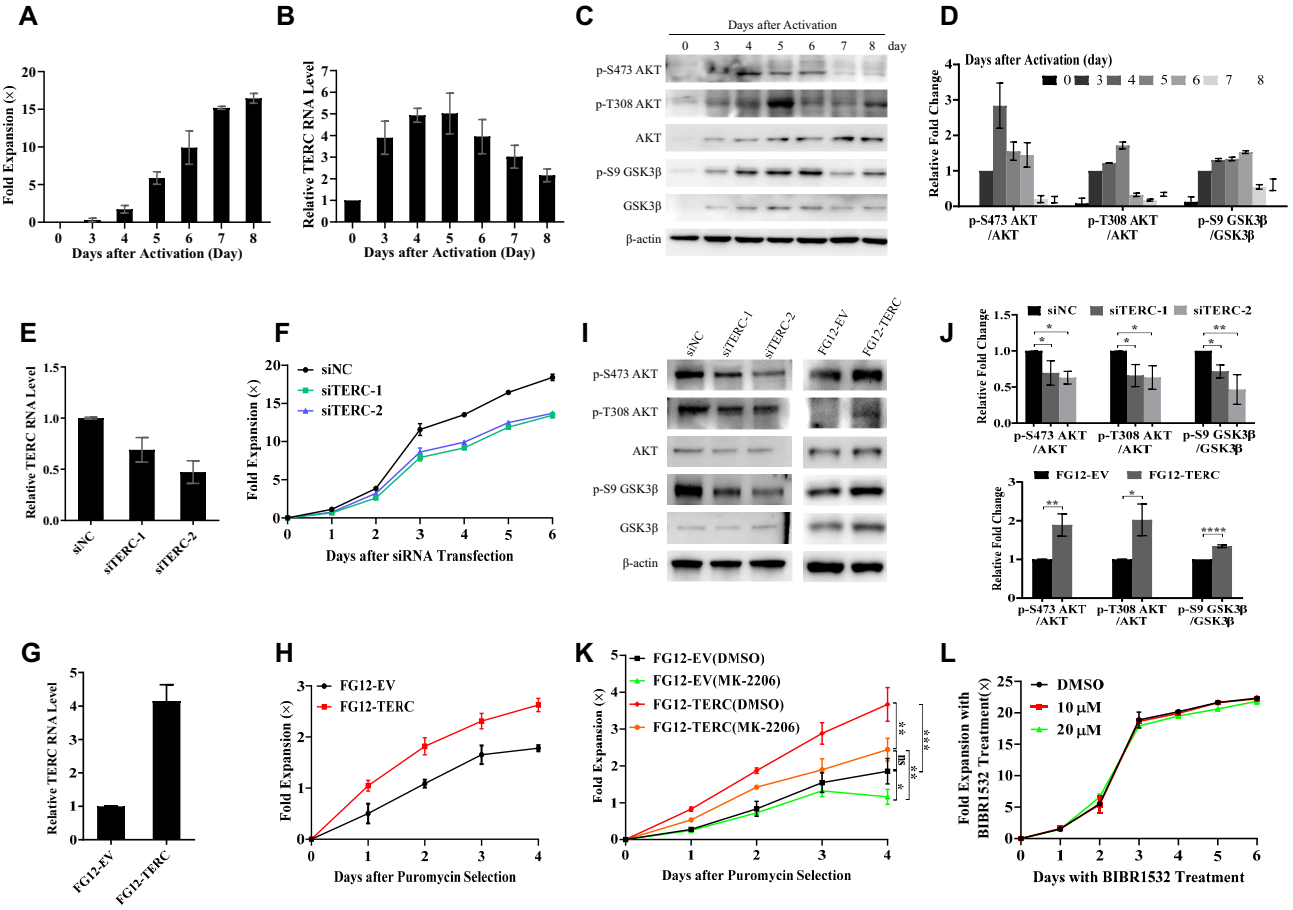

Figure 5. TERC elevates the proliferation of activated CD4$^+$ T cells through activating AKT in a telomerase activity-independent manner. (**A**) Fold expansion of peripheral blood CD4$^+$ T cells after *in vitro* activation. Negatively selected-CD4$^+$ T cells were activated with ImmunoCult Human CD3/CD28 T Cell Activator in ImmunoCult™-XF T Cell Expansion Medium supplemented with 10 ng/ml IL-2, on days 0, 3, 4, 5, 6, 7 and 8, viable cells were counted and fold expansion was calculated. (**B**) TERC RNA level was increased in peripheral blood CD4$^+$ T cells after in vitro activation. Cells were activated as shown in (A), on days 0, 3, 4, 5, 6, 7 and 8, cells were collected for RNA extraction, qPCR analysis of TERC expression. (**C**) AKT was activated in peripheral blood CD4$^+$ T cells after *in vitro* activation. Cells were activated as shown in (A), on days 0, 3, 4, 5, 6, 7 and 8, cells were collected for western blotting of indicated proteins. (**D**) Quantification of the data in (C), data represent the mean ± SD of three independent experiments. (**E**) The RNA level of TERC in the control and the TERC-depleted activated CD4$^+$ T cells. Naïve CD4$^+$ T cells were activated with ImmunoCult Human CD3/CD28 T Cell Activator for 3 days followed by transfecting with two distinct siRNAs target to TERC for 6 days, qPCR analysis of TERC knockdown efficiency. (**F**) Proliferation of the control and the TERC-depleted activated CD4$^+$ T cells. Activated CD4$^+$ T cells were transfected with siRNAs for 6 days, viable cells were counted and fold expansion was calculated. (**G**) The RNA level of TERC in the control and the TERC-overexpressed activated CD4$^+$ T cells. Naïve CD4$^+$ T cells were activated with ImmunoCult Human CD3/CD28 T Cell Activator for 3 days followed by lentivirus infection (FG12-Vector or FG12-TERC) for 24 hours, and selected with puromycin for 24 h, qPCR analysis of TERC overexpression efficiency. (**H**) Proliferation of the control and the TERC-overexpressed activated CD4$^+$ T cells. Activated CD4$^+$ T cells were treated as shown in (G), and the TERC-stably expressed activated CD4$^+$ T cells were constructed after puromycin selection, viable cells were counted and fold expansion was calculated. (**I**) TERC depletion decreased AKT activation and TERC overexpression induced AKT activation in activated CD4$^+$ T cells. The control and the TERC-depleted or -overexpressed activated CD4$^+$ T cells were collected for western blotting of indicated proteins. (**J**) Quantification of the data in (I), data represent the mean ± SD of three independent experiments, significance was determined using one-way ANOVA with Dunnett's test or two-tailed Student's *t*-test. TERC knockdown: for p-S473 AKT/AKT: $*P = 0.0250$ (siTERC-1) and 0.0107 (siTERC-2) compared with siNC; for p-S308 AKT/AKT: $*P = 0.0313$ (siTERC-1) and 0.0231 (siTERC-2) compared with siNC; for p-S9 GSK3β/GSK3β: $*P = 0.0308$, $**P = 0.0029$. TERC overexpression: for p-S473 AKT/AKT: $**P = 0.0058$; for p-S308 AKT/AKT: $*P = 0.0123$; for p-S9 GSK3β/GSK3β: $****P < 0.0001$. (**K**) MK-2206 rescued TERC overexpression-induced cell proliferation. Activated CD4$^+$ T cells with EV or TERC stable overexpression were constructed, and treated with DMSO, MK-2206 (an AKT inhibitor, 2.5 μM) for 4 days, viable cells were counted and fold expansion was calculated. Data represent the mean ± SD of three independent experiments, significance was determined using two-way ANOVA with Tukey's test, $*P = 0.0399$, $**P = 0.0099$ (FG12-TERC(DMSO) versus FG12-TERC(MK-2206)) and 0.0075 (FG12-EV(MK-2206) versus FG12-TERC(MK-2206)), $***P = 0.0008$, ns = 0.2283. (**L**) Proliferation of DMSO and BIBR1352-treated activated CD4$^+$ T cells. Activated CD4$^+$ T cells were treated with DMSO or BIBR1352 for 6 days, viable cells were counted and fold expansion was calculated.

influence of telomerase activity on the proliferation of activated CD4$^+$ T cells, we treated activated CD4$^+$ T cells with BIBR 1532 and found that BIBR 1532 significantly blocked telomerase activity but did not result in inhibition of cell proliferation (Figure 5L and Supplementary Figure S5A). Importantly, no significant changes were detected in the level of activated AKT or the expression of TERC and TERT with BIBR 1532 treatment (Supplementary Figure S5B–D). Moreover, we observed that TERC-induced cell proliferation and AKT activation could not be reversed by BIBR 1532 treatment (Supplementary Figure S6). These results further confirmed that TERC regulates the proliferation of activated CD4$^+$ T cells independent of telomerase activity.

DISCUSSION

TERC is the core subunit of telomerase which is responsible for adding telomeric sequences to the telomere ends. In addition to being the RNA template of telomerase, TERC is a typical lncRNA and is ubiquitously expressed in normal somatic cells without telomerase activity (5–7). It is very likely that TERC has other, yet to be discovered functions in normal somatic cells. In this study, we demonstrated that TERC elevates cell proliferation independent of telomerase activity by transcriptional regulation of target genes from the PI3K-AKT signaling pathway. Furthermore, we found that the key transcription factor FOXO1, which is negatively regulated by the PI3K-AKT pathway, transcriptionally suppresses TERC expression. These results demonstrate a novel positive feedback loop between TERC and the PI3K-AKT pathway (Figure 6). Intriguingly, TERC-induced AKT activation was found to be critical for the proliferation of activated CD4$^+$ T cells, revealing a potential role of TERC in elevating adaptive immune reactions. Collectively, this newly identified TERC/targeted-genes/AKT/FOXO1/TERC positive feedback loop not only expands the noncanonical function of TERC besides via telomerase activity, but also suggests a novel strategy for elevating adaptive immune reactions to defend against infectious pathogens and tumor cells.

Previously, TERC was considered as a nonfunctional lncRNA waiting for TERT to form the catalytic telomerase complex. However, recent studies have shown that TERC has noncanonical functions that are involved in immune cell antiapoptotic effects and the DNA damage response independent of telomerase activity (8–10). In this study, we identified a novel function of TERC in regulating cell proliferation in normal somatic cells via a positive feedback loop with the PI3K-AKT pathway which has been revealed to be involved in cell proliferation. Interestingly, the PI3K-AKT pathway has been reported to contribute to cell survival and genomic integrity maintenance (48). Prior studies have also revealed that there is a crosstalk between the PI3K-AKT pathway and the DNA damage response in cells (49–51). These observations lead to the intriguing possibility that the PI3K-AKT pathway may act as the key intermediate signaling pathway for TERC to exert its reported noncanonical functions. Moreover, the PI3K-AKT pathway plays critical roles in various other biological processes, such as cell metabolism, protein synthesis and angiogenesis (14,15). Whether TERC is also involved in these processes independent of telomerase activity requires further investigation.

While identifying the genomic occupancy of TERC helps to understand its functional mechanism on chromosomal DNA. It has been reported that TERC occupies telomeres and some of the same genes as TERT does in HeLa S3 cells transfected with TERC and TERT (23). However, the genomic targets of TERC in cells, especially in TERT-negative cells, are unclear. Analysis of TERC ChIRP-seq in MRC5 fibroblast cells, we did not observe an apparent enrichment of TERC on telomeres (Figure 2B), further supporting that TERT aids the recruitment of TERC to telomeres (34). Moreover, we showed that TERC preferentially targets gene promoters/transcriptional start sites, which is consistent with the re-analyzed results of ChIRP-seq in HeLa S3 cells (11,23). Further KEGG pathway analysis revealed that the gene targets of TERC in fibroblast cells were enriched in the PI3K-AKT pathway, which provides mechanistic insight into the function of TERC on transcriptional regulation in normal somatic cells. With experimental confirmation, we demonstrated that three genes (EGFR, IL4R, PDPK1) from the PI3K-AKT pathway are transcriptionally induced by TERC (Figure 3B–D), giving the explanation that TERC-depletion cells present lower level of activated AKT than control cells. Intriguingly, we also showed that activated AKT can elevate TERC expression through FOXO1, a key transcription factor, which is negatively regulated by the PI3K-AKT pathway (Figure 4). Therefore, our study identified a positive feedback loop between the PI3K-AKT pathway and TERC.

Unsurprisingly, KEGG pathway analysis of TERC-ChIRP seq in MRC5 cells showed that the highest number of TERC-occupied genes were enriched in 'Pathways in cancer' (Figure 2F), and we also revealed that TERC overexpression induces AKT activation and EGFR expression. It is proposed that abnormal overexpression of activated AKT and EGFR is commonly observed in many cancers and is highly correlated with advanced stage of disease and poor prognosis (52–55). This observation suggested that in addition to acting as the RNA template for telomerase to maintain telomeres in cancer cells, TERC-induced AKT activation and EGFR expression may provide another molecular explanation for the critical role of TERC in cancer progression. Currently, AKT and EGFR are considered as the attractive targets for cancer therapy and prevention. TERC depletion significantly inhibits AKT activation and EGFR expression independent of telomerase activity, revealing that depletion of TERC in tumor cells can be utilized as a cancer therapeutic strategy. Our future studies will investigate these interesting questions. However, KEGG pathway analysis in our study cannot enrich the NF-κB pathway which has been reported to be activated by TERC in U2OS (a cancer cell line) independent of telomerase activity (11). One obvious reason for this discrepancy can be that the NF-κB pathway has been reported to be persistently activated in various malignancies (56,57) but tightly regulated and only can be activated with external stimuli in normal cells (58,59). So it hardly be enriched in MRC5 (a normal somatic cell line) without any stimuli in our study. Further experiments are required to establish the

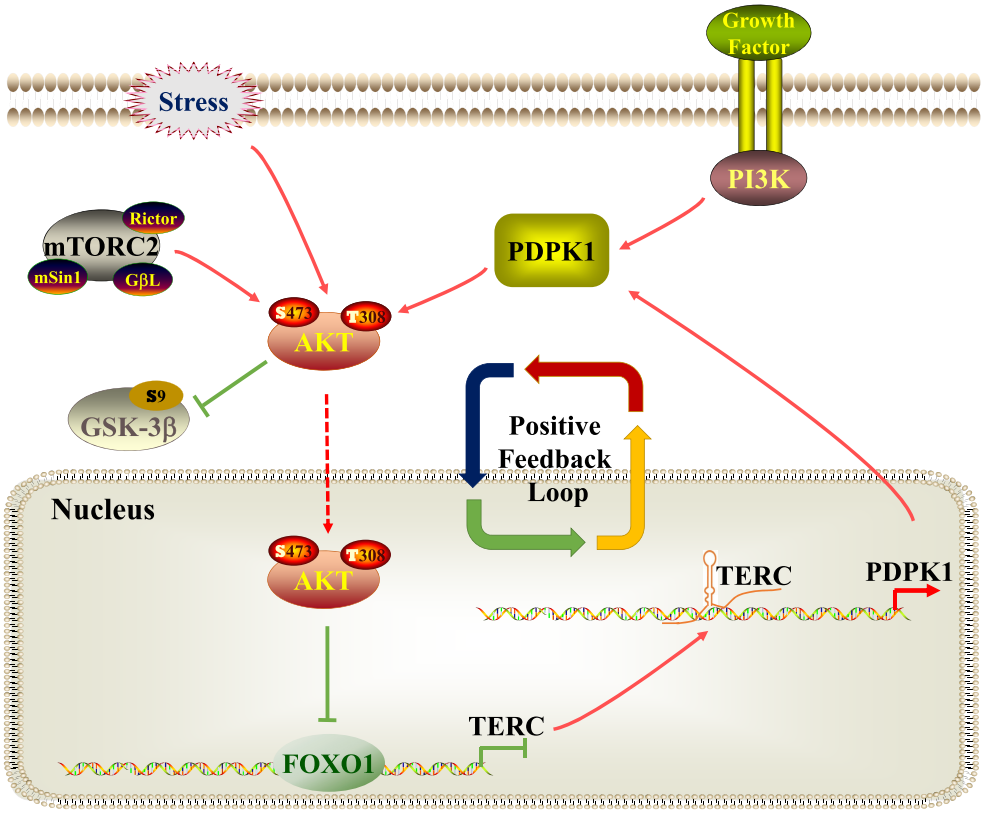

Figure 6. Proposed working model for TERC to regulate cell proliferation independent of telomerase activity via the positive feedback loop with the PI3K-AKT pathway (see text for details).

different functions of TERC in cancer cells and normal somatic cells.

CD4$^+$ T cells have been reported to play central roles in adaptive immunity, driving appropriate immune responses to diverse types of invading pathogens. Monitoring CD4$^+$ T cell proliferation is essential for the evaluation of adaptive immune reactions (40). A prior study showed that TERC protects activated CD4$^+$ T cells from apoptosis independent of telomerase integrity and enzymatic activity (8), but the mechanism is not clear. Here, we showed that TERC positively regulates the PI3K-AKT signaling pathway in activated CD4$^+$ T cells, which might be important for TERC to protect cells from apoptosis. Recently, it has been reported that telomerase activity is not required for the short-term proliferation of activated T cells (60), which is consistent with our results that the proliferation rate of activated CD4$^+$ T cells was unaffected with BIBR 1532 treatment which can significantly inhibit telomerase activity (Figure 5L and Supplementary Figure S5). Importantly, we demonstrated that TERC is a prominent regulator for the proliferation of activated CD4$^+$ T cells and this function is independent of telomerase activity. Furthermore, another report revealed that PD-1 signaling inhibits T cell activation through preventing CD28-mediated activation of PI3K-induced AKT phosphorylation (61). Thus, supplementation with TERC in T cells may override PD-1-inhibited T cell activation to improve the function of T cells in cancer therapy. It is possible that we can elevate adaptive immune reactions through altering TERC level in primary human immune cells to defend against infectious pathogens and tumor cells.

DATA AVAILABILITY

The raw ChIRP-seq data has been submitted to GEO database. The GEO accession link is https://www.ncbi.nlm.nih.gov/geo/query/acc.cgi?acc=GSE183642. All other data are available from the corresponding author upon reasonable request.

SUPPLEMENTARY DATA

Supplementary Data are available at NAR Online.

ACKNOWLEDGEMENTS

Regretfully, Prof. Yong Zhao passed away during the research period. We dedicate this article to his memory. We thank all the members in Prof. Zhao's laboratory and Prof. Ju's laboratory for insightful scientific discussion.

Author Contributions: S.W., Y.G. and Y.Z. initiated the study and generated the hypotheses. S.W., Z.J. and Y.G. designed and performed experiments with the help of Q.L., and H.Z., S.W. and K.L. analyzed ChIRP-seq data. S.W., Y.G., W.H. and Z.J. analyzed and interpreted the experimental data. S.W., Y.G., W.H. and Z.J. wrote the manuscript with the help of K.L. and Q.H., W.H. and Z.J. supervised this project. All authors read and approved the submission of this manuscript.

FUNDING

National Key R&D Program of China [2021YFA0804903, 2021YFA1100103]; National Natural Science Foundation of China [82030039, 32000602, 92049304]; Guangdong Basic and Applied Basic Research Foundation [2020A1515011522, 2020A1515110479]; Fundamental Research Funds for the Central Universities [21620431]; Open Project of the State Key Laboratory of Trauma, Burn and Combined Injury, Third Military Medical University [SKLKF202002]. Funding for open access charge: National Key R&D Program of China.

Conflict of interest statement. None declared.

REFERENCES

1. Wellinger,R.J. (2014) In the end, what's the problem?*Mol. Cell*, **53**, 855–856.
2. Morin,G.B. (1989) The human telomere terminal transferase enzyme is a ribonucleoprotein that synthesizes TTAGGG repeats. *Cell*, **59**, 521–529.
3. Blackburn,E.H. and Collins,K. (2011) Telomerase: an RNP enzyme synthesizes DNA. *Cold Spring Harb. Perspect. Biol.*, **3**, a003558.
4. Nandakumar,J. and Cech,T.R. (2013) Finding the end: recruitment of telomerase to telomeres. *Nat. Rev. Mol. Cell Biol.*, **14**, 69–82.
5. Cong,Y.S., Wright,W.E. and Shay,J.W. (2002) Human telomerase and its regulation. *Microbiol. Mol. Biol. Rev.*, **66**, 407–425.
6. Ito,H., Kyo,S., Kanaya,T., Takakura,M., Inoue,M. and Namiki,M. (1998) Expression of human telomerase subunits and correlation with telomerase activity in urothelial cancer. *Clin. Cancer Res.*, **4**, 1603–1608.
7. Takakura,M., Kyo,S., Kanaya,T., Tanaka,M. and Inoue,M. (1998) Expression of human telomerase subunits and correlation with telomerase activity in cervical cancer. *Cancer Res.*, **58**, 1558–1561.
8. Gazzaniga,F.S. and Blackburn,E.H. (2014) An antiapoptotic role for telomerase RNA in human immune cells independent of telomere integrity or telomerase enzymatic activity. *Blood*, **124**, 3675–3684.
9. Kedde,M., le Sage,C., Duursma,A., Zlotorynski,E., van Leeuwen,B., Nijkamp,W., Beijersbergen,R. and Agami,R. (2006) Telomerase-independent regulation of ATR by human telomerase RNA. *J. Biol. Chem.*, **281**, 40503–40514.
10. Ting,N.S., Pohorelic,B., Yu,Y., Lees-Miller,S.P. and Beattie,T.L. (2009) The human telomerase RNA component, hTR, activates the DNA-dependent protein kinase to phosphorylate heterogeneous nuclear ribonucleoprotein a1. *Nucleic Acids Res.*, **37**, 6105–6115.
11. Liu,H., Yang,Y., Ge,Y., Liu,J. and Zhao,Y. (2019) TERC promotes cellular inflammatory response independent of telomerase. *Nucleic Acids Res.*, **47**, 8084–8095.
12. Zheng,Q., Liu,P., Gao,G., Yuan,J., Wang,P., Huang,J., Xie,L., Lu,X., Di,F., Tong,T. *et al.* (2019) Mitochondrion-processed TERC regulates senescence without affecting telomerase activities. *Protein Cell*, **10**, 631–648.
13. Cheng,Y., Liu,P., Zheng,Q., Gao,G., Yuan,J., Wang,P., Huang,J., Xie,L., Lu,X., Tong,T. *et al.* (2018) Mitochondrial trafficking and processing of telomerase RNA TERC. *Cell Rep.*, **24**, 2589–2595.
14. Xie,Y., Shi,X., Sheng,K., Han,G., Li,W., Zhao,Q., Jiang,B., Feng,J., Li,J. and Gu,Y. (2019) PI3K/Akt signaling transduction pathway, erythropoiesis and glycolysis in hypoxia (Review). *Mol. Med. Rep.*, **19**, 783–791.
15. Keppler-Noreuil,K.M., Parker,V.E., Darling,T.N. and Martinez-Agosto,J.A. (2016) Somatic overgrowth disorders of the PI3K/AKT/mTOR pathway & therapeutic strategies. *Am. J. Med. Genet. C Semin. Med. Genet.*, **172**, 402–421.
16. Goldbraikh,D., Neufeld,D., Eid-Mutlak,Y., Lasry,I., Gilda,J.E., Parnis,A. and Cohen,S. (2020) USP1 deubiquitinates akt to inhibit PI3K-Akt-FoxO signaling in muscle during prolonged starvation. *EMBO Rep.*, **21**, e48791.
17. Manning,B.D. and Toker,A. (2017) AKT/PKB signaling: navigating the network. *Cell*, **169**, 381–405.
18. Cantley,L.C. (2002) The phosphoinositide 3-kinase pathway. *Science (New York, N.Y.)*, **296**, 1655–1657.
19. Alessi,D.R., James,S.R., Downes,C.P., Holmes,A.B., Gaffney,P.R., Reese,C.B. and Cohen,P. (1997) Characterization of a 3-phosphoinositide-dependent protein kinase which phosphorylates and activates protein kinase balpha. *Curr. Biol.: CB*, **7**, 261–269.
20. Sarbassov,D.D., Guertin,D.A., Ali,S.M. and Sabatini,D.M. (2005) Phosphorylation and regulation of Akt/PKB by the rictor-mTOR complex. *Science (New York, N.Y.)*, **307**, 1098–1101.
21. Qin,X.F., An,D.S., Chen,I.S. and Baltimore,D. (2003) Inhibiting HIV-1 infection in human t cells by lentiviral-mediated delivery of small interfering RNA against CCR5. *Proc. Nat. Acad. Sci. U.S.A.*, **100**, 183–188.
22. Wong,J.M. and Collins,K. (2006) Telomerase RNA level limits telomere maintenance in X-linked dyskeratosis congenita. *Genes Dev.*, **20**, 2848–2858.
23. Chu,C., Qu,K., Zhong,F.L., Artandi,S.E. and Chang,H.Y. (2011) Genomic maps of long noncoding RNA occupancy reveal principles of RNA-chromatin interactions. *Mol. Cell*, **44**, 667–678.
24. Chu,C., Quinn,J. and Chang,H.Y. (2012) Chromatin isolation by RNA purification (ChIRP). *J. Visual. Experim.*, **61**, e3912.
25. Langmead,B. and Salzberg,S.L. (2012) Fast gapped-read alignment with bowtie 2. *Nat. Methods*, **9**, 357–359.
26. Ramírez,F., Ryan,D.P., Grüning,B., Bhardwaj,V., Kilpert,F., Richter,A.S., Heyne,S., Dündar,F. and Manke,T. (2016) deepTools2: a next generation web server for deep-sequencing data analysis. *Nucleic Acids Res.*, **44**, W160–W165.
27. Shin,H., Liu,T., Manrai,A.K. and Liu,X.S. (2009) CEAS: cis-regulatory element annotation system. *Bioinformatics*, **25**, 2605–2606.
28. Huang da,W., Sherman,B.T. and Lempicki,R.A. (2009) Bioinformatics enrichment tools: paths toward the comprehensive functional analysis of large gene lists. *Nucleic Acids Res.*, **37**, 1–13.
29. Huang da,W., Sherman,B.T. and Lempicki,R.A. (2009) Systematic and integrative analysis of large gene lists using DAVID bioinformatics resources. *Nat. Protoc.*, **4**, 44–57.
30. Stelzer,G., Rosen,N., Plaschkes,I., Zimmerman,S., Twik,M., Fishilevich,S., Stein,T.I., Nudel,R., Lieder,I., Mazor,Y. *et al.* (2016) The genecards suite: from gene data mining to disease genome sequence analyses. *Curr. Protoc. Bioinform.*, **54**, 1.30.1–1.30.33.
31. Shay,J.W. and Bacchetti,S. (1997) A survey of telomerase activity in human cancer. *Eur. J. Cancer (Oxford, England: 1990)*, **33**, 787–791.
32. Zhao,Y., Abreu,E., Kim,J., Stadler,G., Eskiocak,U., Terns,M.P., Terns,R.M., Shay,J.W. and Wright,W.E. (2011) Processive and distributive extension of human telomeres by telomerase under homeostatic and nonequilibrium conditions. *Mol. Cell*, **42**, 297–307.
33. García-Castillo,J., Alcaraz-Pérez,F., Martínez-Balsalobre,E., García-Moreno,D., Rossmann,M.P., Fernández-Lajarín,M., Bernabé-García,M., Pérez-Oliva,A.B., Rodríguez-Cortez,V.C., Bueno,C. *et al.* (2021) Telomerase RNA recruits RNA polymerase II to target gene promoters to enhance myelopoiesis. *Proc. Nat. Acad. Sci. U.S.A.*, **118**, e2015528118.
34. Tomlinson,R.L., Abreu,E.B., Ziegler,T., Ly,H., Counter,C.M., Terns,R.M. and Terns,M.P. (2008) Telomerase reverse transcriptase is required for the localization of telomerase RNA to cajal bodies and telomeres in human cancer cells. *Mol. Biol. Cell*, **19**, 3793–3800.
35. Han,F., Li,C.F., Cai,Z., Zhang,X., Jin,G., Zhang,W.N., Xu,C., Wang,C.Y., Morrow,J., Zhang,S. *et al.* (2018) The critical role of AMPK in driving akt activation under stress, tumorigenesis and drug resistance. *Nat. Commun.*, **9**, 4728.
36. Dreos,R., Ambrosini,G., Groux,R., Cavin Périer,R. and Bucher,P. (2017) The eukaryotic promoter database in its 30th year: focus on non-vertebrate organisms. *Nucleic Acids Res.*, **45**, D51–D55.
37. Brunet,A., Bonni,A., Zigmond,M.J., Lin,M.Z., Juo,P., Hu,L.S., Anderson,M.J., Arden,K.C., Blenis,J. and Greenberg,M.E. (1999) Akt promotes cell survival by phosphorylating and inhibiting a forkhead transcription factor. *Cell*, **96**, 857–868.
38. Tang,E.D., Nuñez,G., Barr,F.G. and Guan,K.L. (1999) Negative regulation of the forkhead transcription factor FKHR by akt. *J. Biol. Chem.*, **274**, 16741–16746.
39. Link,W. (2019) Introduction to FOXO biology. *Methods Mol. Biol.*, **1890**, 1–9.
40. Luckheeram,R.V., Zhou,R., Verma,A.D. and Xia,B. (2012) $CD4^+$T cells: differentiation and functions. *Clin. Dev. Immunol.*, **2012**, 925135.
41. Weng,N., Levine,B.L., June,C.H. and Hodes,R.J. (1997) Regulation of telomerase RNA template expression in human t lymphocyte

development and activation. *J. Immunol. (Baltimore, Md. : 1950)*, **158**, 3215–3220.
42. Pagès,F., Ragueneau,M., Rottapel,R., Truneh,A., Nunes,J., Imbert,J. and Olive,D. (1994) Binding of phosphatidylinositol-3-OH kinase to CD28 is required for T-cell signalling. *Nature*, **369**, 327–329.
43. Ward,S.G., Westwick,J., Hall,N.D. and Sansom,D.M. (1993) Ligation of CD28 receptor by B7 induces formation of D-3 phosphoinositides in t lymphocytes independently of t cell receptor/CD3 activation. *Eur. J. Immunol.*, **23**, 2572–2577.
44. Franchina,D.G., Dostert,C. and Brenner,D. (2018) Reactive oxygen species: involvement in t cell signaling and metabolism. *Trends Immunol.*, **39**, 489–502.
45. Lian,G., Gnanaprakasam,J.R., Wang,T., Wu,R., Chen,X., Liu,L., Shen,Y., Yang,M., Yang,J., Chen,Y. *et al.* (2018) Glutathione de novo synthesis but not recycling process coordinates with glutamine catabolism to control redox homeostasis and directs murine t cell differentiation. *Elife*, **7**, e36158.
46. El-Daly,H., Kull,M., Zimmermann,S., Pantic,M., Waller,C.F. and Martens,U.M. (2005) Selective cytotoxicity and telomere damage in leukemia cells using the telomerase inhibitor BIBR1532. *Blood*, **105**, 1742–1749.
47. Röth,A., Dürig,J., Himmelreich,H., Bug,S., Siebert,R., Dührsen,U., Lansdorp,P.M. and Baerlocher,G.M. (2007) Short telomeres and high telomerase activity in T-cell prolymphocytic leukemia. *Leukemia*, **21**, 2456–2462.
48. Maidarti,M., Anderson,R.A. and Telfer,E.E. (2020) Crosstalk between PTEN/PI3K/Akt signalling and DNA damage in the oocyte: implications for primordial follicle activation, oocyte quality and ageing. *Cells*, **9**, 200.
49. Karimian,A., Mir,S.M., Parsian,H., Refieyan,S., Mirza-Aghazadeh-Attari,M., Yousefi,B. and Majidinia,M. (2019) Crosstalk between phosphoinositide 3-kinase/Akt signaling pathway with DNA damage response and oxidative stress in cancer. *J. Cell. Biochem.*, **120**, 10248–10272.
50. Plo,I., Laulier,C., Gauthier,L., Lebrun,F., Calvo,F. and Lopez,B.S. (2008) AKT1 inhibits homologous recombination by inducing cytoplasmic retention of BRCA1 and RAD51. *Cancer Res.*, **68**, 9404–9412.
51. Puc,J., Keniry,M., Li,H.S., Pandita,T.K., Choudhury,A.D., Memeo,L., Mansukhani,M., Murty,V.V., Gaciong,Z., Meek,S.E. *et al.* (2005) Lack of PTEN sequesters CHK1 and initiates genetic instability. *Cancer Cell*, **7**, 193–204.
52. Song,M., Bode,A.M., Dong,Z. and Lee,M.H. (2019) AKT as a therapeutic target for cancer. *Cancer Res.*, **79**, 1019–1031.
53. Dias,F., Teixeira,A.L., Santos,J.I., Gomes,M., Nogueira,A., Assis,J. and Medeiros,R. (2013) Renal cell carcinoma development and miRNAs: a possible link to the EGFR pathway. *Pharmacogenomics*, **14**, 1793–1803.
54. Stumm,G., Eberwein,S., Rostock-Wolf,S., Stein,H., Pomer,S., Schlegel,J. and Waldherr,R. (1996) Concomitant overexpression of the EGFR and erbB-2 genes in renal cell carcinoma (RCC) is correlated with dedifferentiation and metastasis. *Int. J. Cancer*, **69**, 17–22.
55. Jänne,P.A., Engelman,J.A. and Johnson,B.E. (2005) Epidermal growth factor receptor mutations in non-small-cell lung cancer: implications for treatment and tumor biology. *J. Clin. Oncol.: Off. J. Am. Soc. Clin. Oncol.*, **23**, 3227–3234.
56. Karin,M. (2006) Nuclear factor-kappaB in cancer development and progression. *Nature*, **441**, 431–436.
57. Zinatizadeh,M.R., Schock,B., Chalbatani,G.M., Zarandi,P.K., Jalali,S.A. and Miri,S.R. (2021) The nuclear factor kappa b (NF-kB) signaling in cancer development and immune diseases. *Genes Dis.*, **8**, 287–297.
58. De Silva,N.S., Anderson,M.M., Carette,A., Silva,K., Heise,N., Bhagat,G. and Klein,U. (2016) Transcription factors of the alternative NF-κB pathway are required for germinal center B-cell development. *Proc. Nat. Acad. Sci. U.S.A.*, **113**, 9063–9068.
59. Yu,H., Lin,L., Zhang,Z., Zhang,H. and Hu,H. (2020) Targeting NF-κB pathway for the therapy of diseases: mechanism and clinical study. *Signal Trans. Target. Ther.*, **5**, 209.
60. Huang,E.E., Tedone,E., O'Hara,R., Cornelius,C., Lai,T.P., Ludlow,A., Wright,W.E. and Shay,J.W. (2017) The maintenance of telomere length in CD28+ t cells during t lymphocyte stimulation. *Sci. Rep.*, **7**, 6785.
61. Parry,R.V., Chemnitz,J.M., Frauwirth,K.A., Lanfranco,A.R., Braunstein,I., Kobayashi,S.V., Linsley,P.S., Thompson,C.B. and Riley,J.L. (2005) CTLA-4 and PD-1 receptors inhibit T-cell activation by distinct mechanisms. *Mol. Cell. Biol.*, **25**, 9543–9553.